Topical GZ21T Inhibits the Growth of Actinic Keratoses in a UVB-Induced Model of Skin Carcinogenesis

Zachary A. Bordeaux[1,2,7], Justin Choi[1,2,7], Gabriella Braun[2], Cole Davis[2], Melika Marani[1], Kevin Lee[1], Christeen Samuel[1], Jackson Adams[2], Reed Windom[2], Anthony Pollizzi[2], Anusha Kambala[1], Hannah Cornman[1], Sriya V. Reddy[1], Weiying Lu[1], Olusola O. Oladipo[1], Martin P. Alphonse[1], Cameron E. West[3,4], Shawn G. Kwatra[1,5,8] and Madan M. Kwatra[2,6,8]

Actinic keratoses (AKs) are premalignant intraepidermal neoplasms that occur as a result of cumulative sun damage. AKs commonly relapse, and up to 16% undergo malignant transformation into cutaneous squamous cell carcinoma. There is a need for novel therapies that reduce the quantity and surface area of AKs as well as prevent malignant transformation to cutaneous squamous cell carcinomas. We recently showed that GZ17-6.02, an anticancer agent composed of curcumin, haramine, and isovanillin, inhibited the growth of H297.T cells. This study evaluated the efficacy of a topical formulation of GZ17-6.02, known as GZ21T, in a murine model of AK generated by exposing SKH1 mice to UVR. Treatment of mice with topical GZ21T inhibited the growth of AKs by decreasing both lesion count ($P = 0.012$) and surface area occupied by tumor ($P = 0.002$). GZ21T also suppressed the progression of AKs to cutaneous squamous cell carcinoma by decreasing the count ($P = 0.047$) and surface area ($P = 0.049$) of lesions more likely to represent cutaneous squamous cell carcinoma. RNA sequencing and proteomic analyses revealed that GZ21T suppressed several pathways, including MAPK ($P = 0.025$), phosphoinositide 3-kinase–protein kinase B ($P = 0.04$), HIF-1α ($P = 0.016$), Wnt ($P = 0.025$), insulin ($P = 0.018$), and ERBB ($P = 0.016$) signaling. GZ21T also upregulated the autophagy-promoting protein AMPK while suppressing proteins such as PD-L1, glutaminase, pAkt1 S473, and eEF2K.

JID Innovations (2023);**3:**100206 doi:10.1016/j.xjidi.2023.100206

INTRODUCTION

Actinic keratoses (AKs) are premalignant intraepidermal neoplasms characterized by keratinocyte (KC) atypia in the basal layer of the epidermis, which carry an estimated prevalence of 28–49% (Berman and Cockerell, 2013; Fernandez Figueras, 2017; Flohil et al., 2013). AKs arise as a result of cumulative sun damage and present as rough, scaly patches; plaques; or papules on an erythematous base (Dirschka et al., 2017), typically affecting sun-exposed areas in older, fair-skinned individuals (Boone et al., 2016; Costa et al., 2015; Fernandez Figueras, 2017; Salmon and Tidman, 2016). Patients with few or isolated AKs are typically treated with lesion-directed therapies such as cryotherapy, laser therapy, or curettage, whereas patients with more diffuse lesions may require field-directed therapies such as 5-fluorouracil, diclofenac, imiquimod, or photodynamic therapy. Furthermore, it is estimated that up to 16% of AKs undergo malignant transformation into cutaneous squamous cell carcinoma (cSCC) (Dirschka et al., 2017). Given the side effect profiles and efficacy of current treatment options, novel therapeutic options for the treatment of AKs are needed (Arenberger and Arenbergerova, 2017; Taute et al., 2017).

This study was undertaken to evaluate GZ12T, the topical formulation of GZ17-6.02, in a murine model of AK. The selection of GZ17-6.02, an anticancer agent composed of curcumin (10% by weight), harmine (13% by weight), and isovanillin (77% by weight) (Ghosh et al., 2019), was based on its activity against a variety of malignancies in vitro and in murine models, including head and neck squamous cell carcinoma, pancreatic ductal adenocarcinoma, melanoma, and glioblastoma (Booth et al., 2022a, 2021; Choi et al., 2022a; Ghosh et al., 2019; Vishwakarma et al., 2018). Finally, our preliminary evaluation of GZ17-6.02's activity against H279.T cells, a fibroblast cell line derived from a patient with AK, showed its efficacy through the modulation of autophagy and cell death (West et al., 2022).

[1]*Department of Dermatology, Johns Hopkins University School of Medicine, Baltimore, Maryland, USA;* [2]*Department of Anesthesiology, Duke University School of Medicine, Durham, South Carolina, USA;* [3]*Genzada Pharmaceuticals, Hutchinson, Kansas, USA;* [4]*US Dermatology Partners, Dallas, Texas, USA;* [5]*Department of Oncology, Johns Hopkins University School of Medicine, Baltimore, Maryland, USA; and* [6]*Department of Pharmacology & Cancer Biology, Duke University School of Medicine, Durham, South Carolina, USA*

[7]*These authors contributed equally to this work.*

[8]*These authors contributed equally as senior authors.*

Correspondence: Shawn G. Kwatra, Department of Dermatology, Johns Hopkins University School of Medicine, Cancer Research Building II, Suite 206, 1550 Orleans Street, Baltimore, Maryland 21231, USA. E-mail: skwatra1@jhmi.edu

Abbreviations: AK, actinic keratosis; Akt, protein kinase B; cSCC, cutaneous squamous cell carcinoma; DEG, differentially expressed gene; GSEA, gene set enrichment analysis; KC, keratinocyte; NL, nonlesional; PI3K, phosphoinositide 3-kinase; PL, perilesional; RPPA, reverse phase protein array

Received 23 October 2022; revised 31 January 2023; accepted 3 March 2023; accepted manuscript published online 6 May 2023; corrected proof published online 19 June 2023

Cite this article as: JID Innovations 2023;3:100206

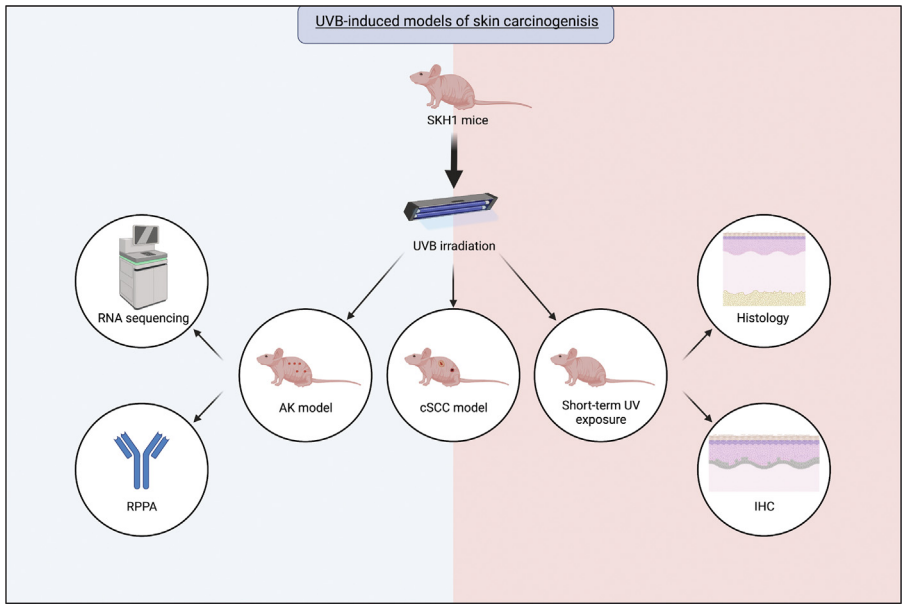

Figure 1. Overall study design. SKH1 mice were used for in vivo models of skin carcinogenesis. Varying UVB exposure protocols were used to evaluate the effects of GZ21T with a model of AK, a model of cSCC, and short-term UV exposure designed to mimic a sunny vacation. RNA sequencing and RPPAs were performed on skin samples from the AK experiments, whereas histology and IHC were performed on the skin from the short-term UV exposure experiments. This figure was created with biorender.com. AK, actinic keratosis; cSCC, cutaneous squamous cell carcinoma; IHC, immunohistochemistry; RPPA, reverse phase protein arrays.

The antitumor activity of GZ17-6.02 appears to be due to the inherent synergism of its components. Curcumin is a well-studied antitumor agent found in the dietary spice turmeric that suppresses tumor progression through the inhibition of pathways such as phosphoinositide 3-kinase (PI3K)—protein kinase B (Akt)/mTOR signaling, which has previously been implicated in the pathogenesis of AK and cSCC (Maiti et al., 2019; Thomson et al., 2021; Vallianou et al., 2015). Curcumin has also been found to activate the tumor suppressor p53 and to suppress EGFR signaling by blocking the binding of EGR-1 to the EGFR promoter and inhibiting the phosphorylation of EGFR (Chen et al., 2006; Sun et al., 2012; Vollono et al., 2019; Zhen et al., 2014). Similarly, harmine is shown to disrupt EGFR signaling by inhibiting DYRK1A (Pozo et al., 2013) and to inhibit Akt/mTOR and extracellular signal—regulated kinase signaling (Chamcheu et al., 2019). Harmine also exerts antitumor activity by inhibiting DNA replication, inducing DNA damage, reducing cell cycle progression, and suppressing angiogenesis (Zhang et al., 2020). Furthermore, the components of GZ17-6.02 appear to be synergistic in their ability to inhibit tumor growth as they have been shown to produce greater cell killing, greater activation of the autophagic flux, and greater inhibition of mitogenic effectors such as mTOR and Akt when administered together than each compound alone or in pairs (Booth et al., 2022b; Bordeaux et al., 2023; Vishwakarma et al., 2018).

In this study, we evaluate the efficacy of topical GZ12T against AK in vivo using a UVB-induced model of skin carcinogenesis. Our results show that GZ21T inhibits AK growth, blocks its progression to cSCC, and exerts a cytoprotective effect with short-term UVB exposure. The underlying mechanism, revealed by transcriptomic and proteomic analyses, involves its action at multiple levels, including the downregulation of pathways previously implicated in the pathogenesis of AK such as MAPK, PI3K—Akt, Wnt, and ERBB signaling as well as inhibition of proteins such as PD-L1, glutaminase, pAkt1 S473, and eEF2K (Brennan et al., 2013; Ratushny et al., 2012).

RESULTS

Topical GZ21T inhibits AK growth in a UVB-induced model of skin carcinogenesis

Figure 1 shows an overview of the overall study design. To assess the ability of topical GZ21T to inhibit AK growth in vivo, we used a UVB-induced model of skin carcinogenesis. An overview of the experimental design is shown in Figure 2a, whereas representative images and histology of AK lesions from control and GZ21T-treated mice after 8 weeks of treatment are shown in Figure 2b and c, respectively. After 8 weeks of treatment, mice receiving GZ21T showed a significant decrease in both lesion count ($P = 0.012$) (Figure 2d) and surface area occupied by tumor ($P = 0.002$) (Figure 2e).

Molecular mechanism of AK progression

To better understand the targets that may be affected by GZ21T, we first performed transcriptomic and proteomic analyses to identify the molecular changes that occur with UVB exposure and progression from healthy skin to AK. Figure 3a provides a heatmap of the differentially expressed genes (DEGs) between lesional, perilesional (PL), nonlesional (NL), and non-UV—exposed skin. Interestingly, progression from non-UV—exposed skin to NL, PL, and lesional tissue resulted in an increasing number of DEGs. Compared with non-UV—exposed skin, NL samples showed 194 DEGs (Figure 3b), PL tissue showed 731 DEGs (Figure 3c), and lesional skin showed 1,502 DEGs (Figure 3d). Of the DEGs, 45 were unique to NL tissue; 208 were unique to PL skin; 994 were unique to lesional samples; and 114 were shared among lesional, PL, and NL skin (Figure 3e).

We next conducted gene set enrichment analyses (GSEAs) comparing NL with non-UV—exposed skin and PL with lesional tissue to identify the pathways altered by UV exposure and progression to AK. UV irradiation upregulated several metabolic and synthetic pathways such as oxidative phosphorylation, proteosome, steroid biosynthesis, and the

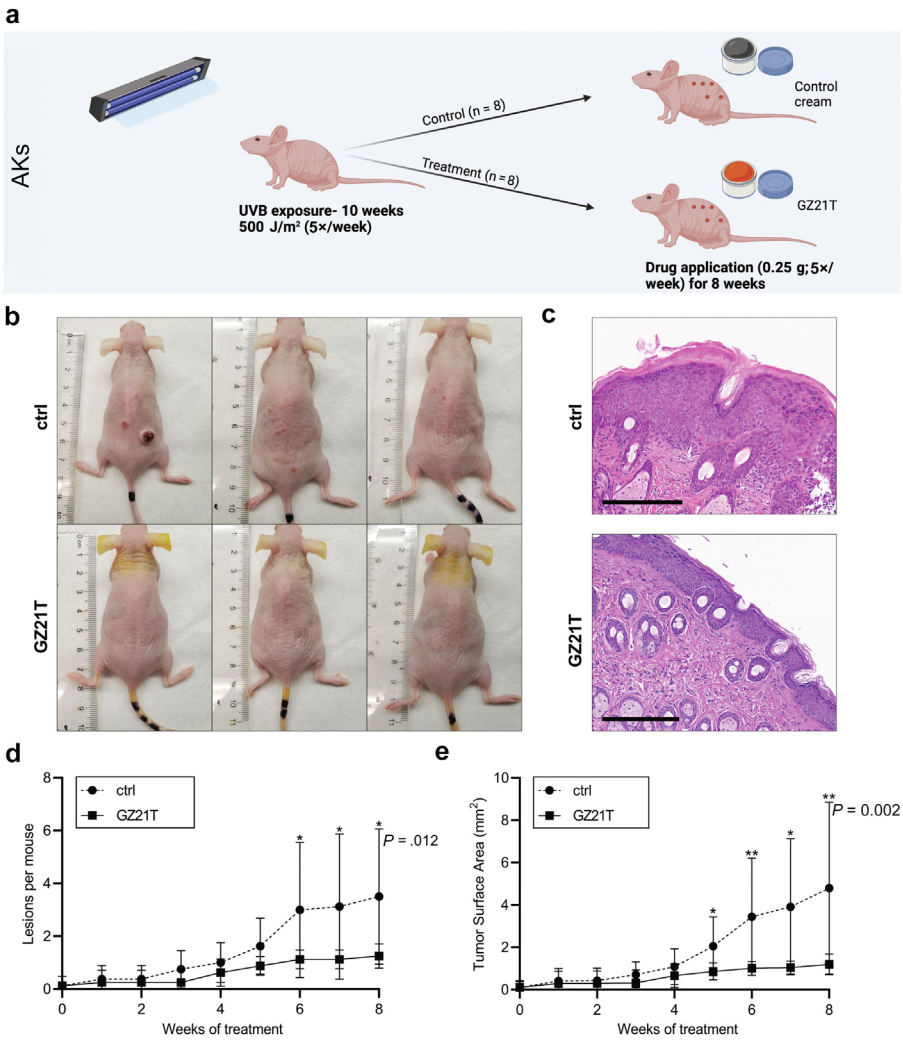

Figure 2. GZ21T inhibits the growth of AKs. (**a**) To induce AK lesions, mice were irradiated with 500 J/m^2 UVB 5 days per week for 10 weeks and were subsequently treated with 0.25 g GZ21T (n = 8) or ctrl cream (n = 8) 5 days per week for 4 weeks. This figure was created with biorender.com. (**b**) Representative images of ctrl and GZ21T-treated mice after 8 weeks of treatment. (**c**) Representative H&E staining of lesional samples from ctrl and GZ21T-treated mice after 8 weeks of treatment. Black bars represent 300 μm. (**d**) Lesion count and (**e**) tumor surface area over time for ctrl and GZ21T-treated mice. Data points represent the mean, whereas error bars represent the SD. *$P < 0.05$. ctrl, control.

tricarboxylic acid cycle (Figure 3f). Progression from PL skin to AK was accompanied by enrichment for pathways involved in DNA synthesis; protein synthesis; and cell cycle progression, such as ribosome, DNA replication, cell cycle, and purine and pyrimidine metabolism (Figure 3g).

Finally, we evaluated the proteomic alterations that occur with UV exposure and progression to AK using reverse phase protein array (RPPA). A comparison of NL and non-UV–exposed skin showed an increase in 20 and a decrease in 23 proteins (Figure 3h). Notably, NL tissue was characterized by upregulation of the T-cell inhibitory protein PD-L1 and glutaminase. A comparison of lesional and PL tissue showed that progression to AK was accompanied by increased expression of nine and decreased expression of nine proteins (Figure 3i). Among the upregulated proteins were pAkt1 S473, a component of the PI3K–Akt signaling pathway, and eEF2K, which supports the survival of neoplastic tissue under conditions of nutrient deprivation (Temme and Asquith, 2021).

Transcriptomic effects of GZ21T treatment

To better understand the mechanism behind GZ21T's anti-tumor activity, we next performed RNA sequencing on lesional skin from control and treated mice. Differential expression analysis revealed 133 DEGs in GZ21T-treated mice, of which 99 were upregulated, and 54 were downregulated (Figure 4a and b). GSEA of GZ21T-treated skin revealed the downregulation of pathways involved in DNA synthesis; protein synthesis; metabolism; and cell cycle progression, such as DNA replication, ribosome, proteasome, oxidative phosphorylation, and cell cycle (Figure 4c). Interestingly, many of these pathways were upregulated by UV exposure and with progression from healthy skin to AK (Figure 3f), indicating that GZ21T may reverse the adverse effects of UV exposure. We next evaluated the effect of GZ21T on pathways previously implicated in the pathogenesis of AK using gene set variation analysis (Thomson et al., 2021). This analysis revealed the suppression of MAPK ($P = 0.025$), PI3K–Akt ($P = 0.040$), HIF-1α ($P = 0.016$), Wnt ($P = 0.025$), insulin ($P = 0.018$), and ERBB ($P = 0.016$) signaling pathways in lesional tissue of GZ21T-treated mice (Figure 4d). Of note, these pathways were not downregulated in NL skin, suggesting that GZ21T may preferentially suppress these targets in neoplastic tissue.

Proteomic effects of GZ21T treatment

We also evaluated the proteins that were altered by GZ21T treatment using RPPA. Figure 5a shows a heatmap of the

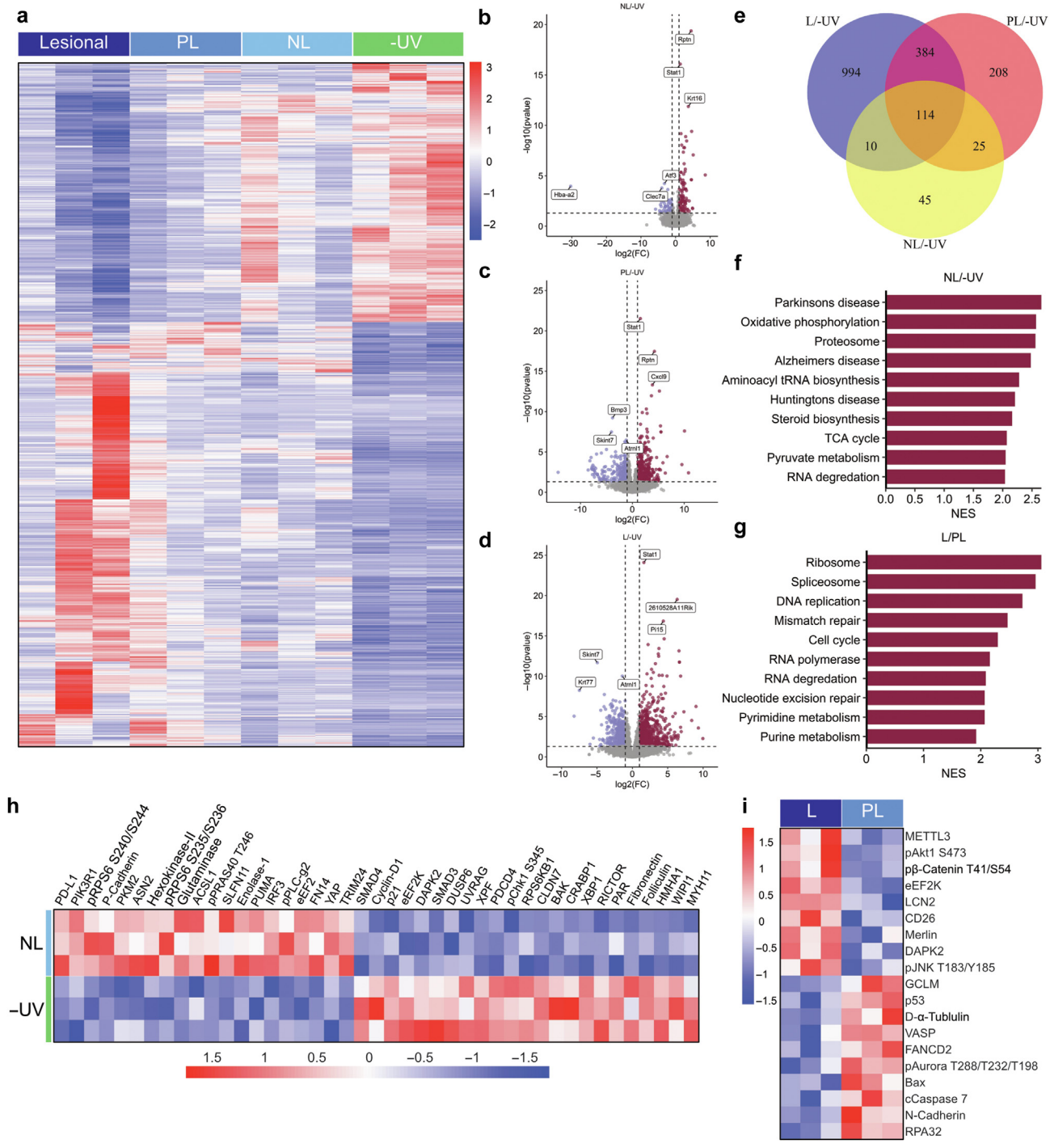

Figure 3. Molecular mechanism of actinic keratoses progression. (**a**) Heatmap of DEGs in lesional, PL, NL, and non-UV–exposed mouse skin. (**b**) Volcano plots for DEGs between NL and non-UV–exposed skin, (**c**) PL and NL skin, and (**d**) lesional and PL skin. (**e**) Venn diagram showing unique and shared DEGs between lesional, PL, and NL skin and non-UV–exposed skin. (**f**) GSEA results for the top pathways enriched in NL compared with those in non-UV–exposed skin and (**g**) lesional compared with those in PL skin. (**h**) Heatmap of differentially expressed proteins between NL and non-UV–exposed skin. (**i**) Differentially expressed proteins between lesional and PL skin. L denotes lesional. DEG, differentially expressed gene; FC, fold change; GSEA, gene set enrichment analysis; NES, normalized enrichment score; NL, nonlesional; PL, perilesional.

significantly different proteins between the lesional skin of control and treated mice, whereas Figure 5b shows the proteins with a change in expression >25% after treatment. Interestingly, GZ21T modulated the expression of several proteins that were altered by UV exposure (Figure 3h). For example, PD-L1 and glutaminase were downregulated, whereas PAR was upregulated. GZ21T also altered the expression of several proteins that we found to be involved in the progression from PL tissue to AK (Figure 3i). Levels of pAkt1 S473, eEF2K, and LCN2 were decreased, whereas those of RPA32 and FANCD2 were increased. We also found that the autophagy-promoting protein, AMPK, was

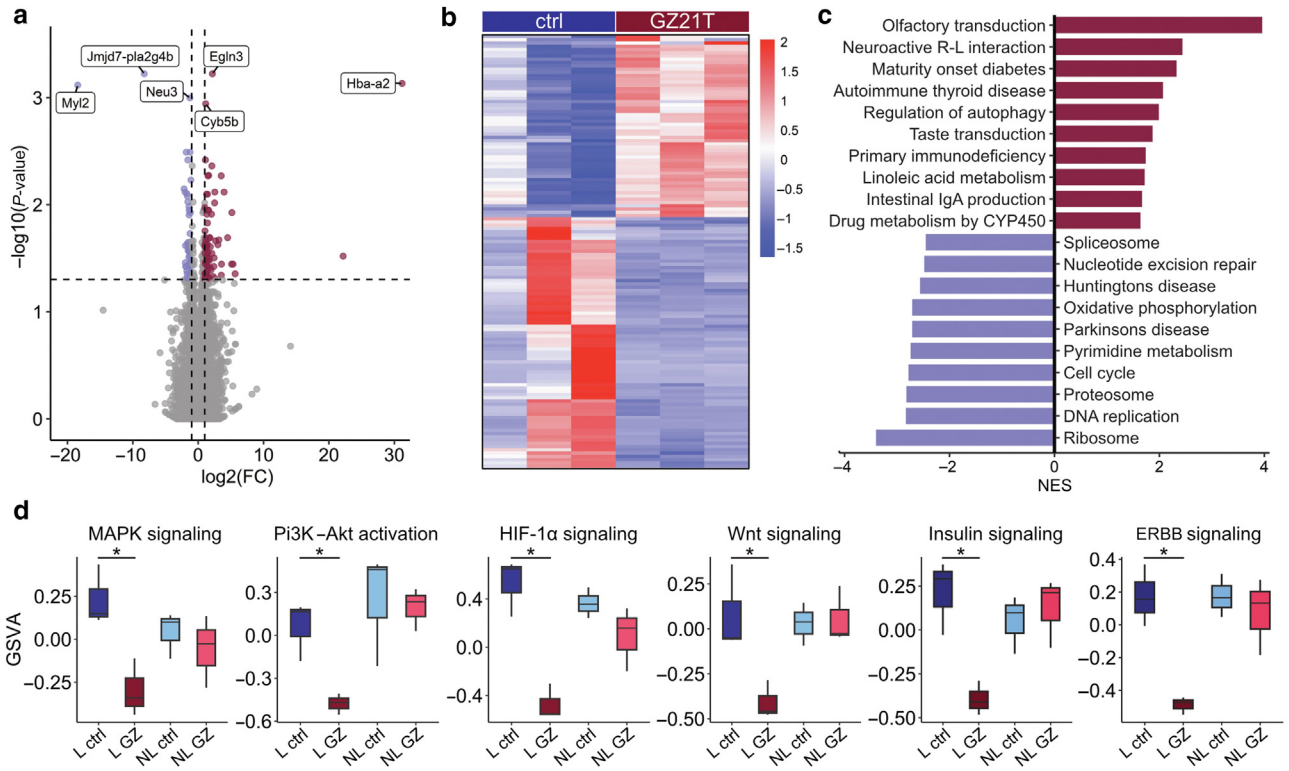

Figure 4. Transcriptomic analysis of control and GZ-treated skin. (**a**) Volcano plot and (**b**) heatmap of DEGs in lesional samples between control and GZ-treated mice. (**c**) GSEA results showing the top pathways upregulated and downregulated by GZ in lesional tissue. (**d**) GSVA for pathways previously implicated in the pathogenesis of AK in lesional and NL tissue from control and GZ-treated mice. Box boundaries represent the interquartile range, with the central line denoting the median and the upper and lower boundaries representing the upper and lower quartiles, respectively. Bars extending above and below box boundaries represent the sample maximum and minimum, respectively. $^*P < 0.05$. L denotes lesional. Akt, protein kinase B; ctrl, control; DEG, differentially expressed gene; FC, fold change; GSVA, gene set variation analysis; GZ, GZ21T; NES, normalized enrichment score; NL, non-lesional; PI3K, phosphoinositide 3-kinase; R-L, receptor−ligand.

upregulated by GZ21T (Li and Chen, 2019). Next, we performed EnrichR functional enrichment analysis on gene lists of proteins downregulated by GZ21T to confirm the alterations in pathways identified by our transcriptomic analysis. Similar to our RNA-sequencing results, this analysis showed suppression of ERBB signaling, cell cycle, insulin signaling, HIF-1α signaling, PI3K−Akt signaling, and MAPK signaling in GZ21T-treated skin (Figure 5c). We also constructed a GeneMANIA network using gene names of proteins downregulated by GZ21T to highlight the genes with shared protein domains and physical interactions or that are colocalized or coexpressed with the targets of GZ21T (Figure 5d). We found that the most over-represented functions of these proteins were related to peptidyl-serine modification, positive regulation of DNA metabolism, cell cycle checkpoints, DNA integrity checkpoints, G2/M phase transition, lymphocyte apoptosis, and the response to UV.

GZ21T prevents the progression of AK to cSCC

We next sought to determine whether GZ21T could prevent the progression of AK to cSCC. To induce cSCC lesions, we prolonged the UV exposure period from 10 weeks in the AK experiment to 14 weeks (Figure 6a). After 6 weeks of treatment, mice were analyzed for the presence of lesions greater than 3 mm in diameter, which are more likely to represent cSCC than AK (de Gruijl and van der Leun, 1991). Representative images of control and GZ21T-treated mice after 6 weeks of treatment are shown in Figure 6b. Analyses of lesions >3 mm in diameter showed a significant decrease in lesion count ($P = 0.047$) (Figure 6c) and surface area covered by tumor ($P = 0.049$) (Figure 6d) in GZ21T-treated mice, suggesting that GZ21T may inhibit the progression of AK to cSCC.

GZ21T is cytoprotective to skin exposed to short-term UVR

We next evaluated the immediate histologic effects of GZ21T treatment with short-term, high-intensity UV exposure designed to mimic a sunny vacation (Figure 7a) (Mintie et al., 2020). Representative H&E images at the end of the UVB exposure period are shown in Figure 7b. Histologic analysis revealed a significant decrease in mean epidermal thickness in the treated group compared with that in control mice (103.9 ± 9.05 μm vs. 157.0 ± 15.32 μm, $P = 0.018$) (Figure 7c). We then assessed the expression of the proliferation marker Ki-67 by immunohistochemistry (Figure 7d). We found a significant decrease in the number of Ki-67−positive cells in the epidermis of treated mice compared with that in the epidermis of the control group (79.6 ± 12.8 per high-powered field vs. 100.02 ± 11.8 per high-powered field, $P = 0.042$) (Figure 7e).

DISCUSSION

We show that topical GZ21T inhibits AK growth in a murine model of skin carcinogenesis. Mechanistically, GZ21T

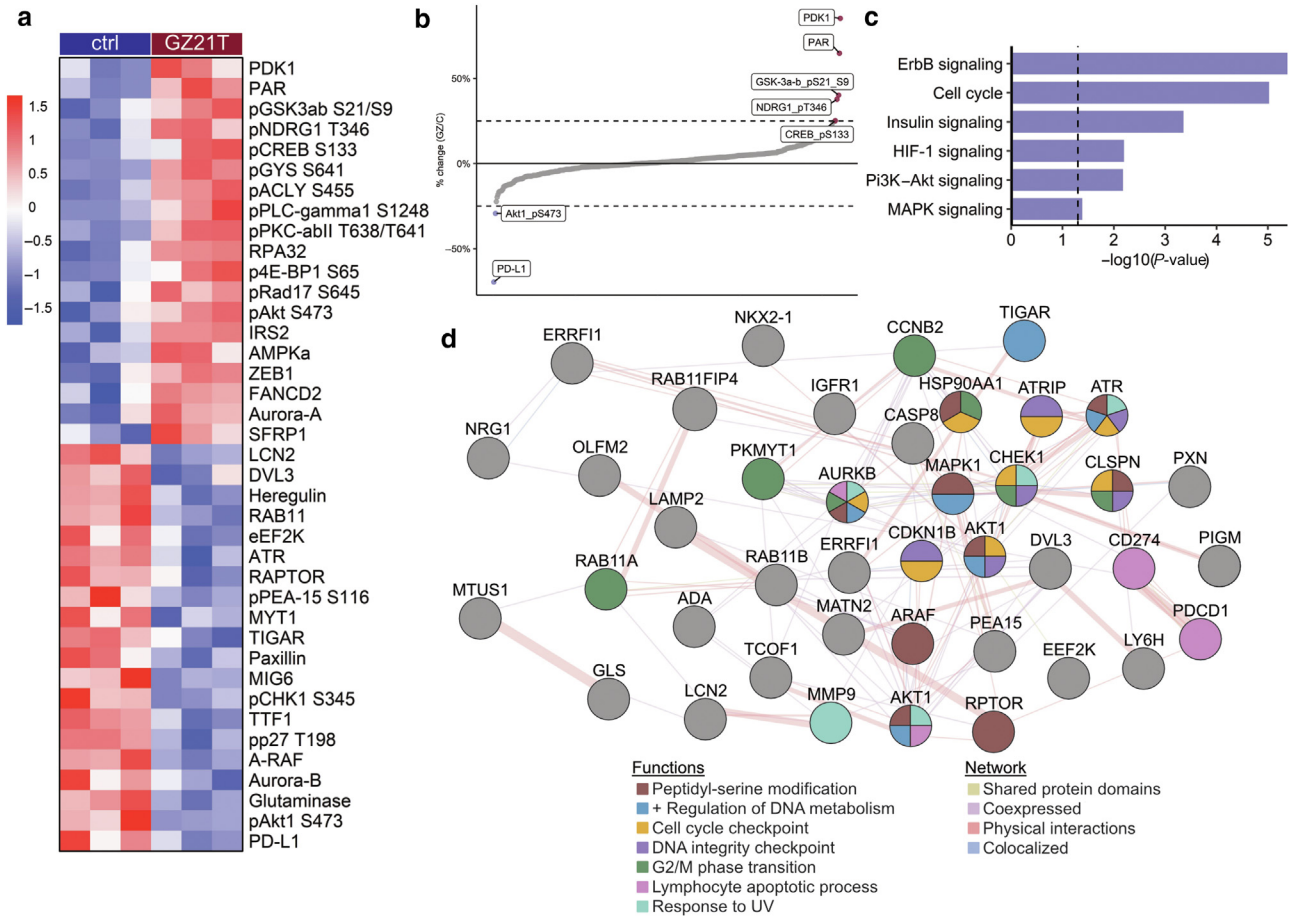

Figure 5. Proteomic analysis of control and GZ21T-treated skin. (**a**) Heatmap of differentially expressed proteins identified by RPPA between lesional samples of control and GZ21T-treated mice. (**b**) Significant proteins showing a percentage change >25% between lesional samples of control and GZ21T-treated mice. (**c**) EnrichR enrichment analysis of proteins downregulated by GZ21T in lesional samples for pathways implicated in the pathogenesis of AK. (**d**) GeneMANIA network of gene lists of proteins downregulated by GZ21T in lesional AK skin. AK, actinic keratosis; Akt, protein kinase B; ctrl, control; PI3K, phosphoinositide 3-kinase; RPPA, reverse phase protein arrays.

downregulates the pathways involved in DNA synthesis, protein synthesis, metabolism, and cell cycle progression. Our results also show that GZ21T prevents the progression of AK to cSCC and exerts cytoprotective activity with short-term UV exposure.

Although previous studies have utilized oral administration or intratumoral injection of GZ17-6.02, this study demonstrates its efficacy in a topical formulation. It is thought that topical administration of curcumin may have superior efficacy to that of oral dosing because the compound is susceptible to a large first-pass metabolism resulting in less than 1% of oral curcumin entering the plasma (Helson, 2013). The topical formulation, GZ21T, can circumvent this drawback because topical medications do not require significant systemic concentrations to reach the skin. Taken together, our findings suggest that the combination of a topical route of administration and the inherent synergism among components of GZ21T makes it an effective drug in the treatment of cutaneous disorders.

In the murine model of skin carcinogenesis, GZ21T was found to be a potent inhibitor of AK growth through its effect on multiple pathways and targets. Transcriptomic analysis of skin from untreated mice showed that progression from PL tissue to AK was accompanied by increases in ribosome, spliceosome, DNA replication, cell cycle, proteasome, and nucleotide excision repair–related processes. These pathways were downregulated by GZ21T treatment.

GZ21T also suppressed several pathways previously implicated in the pathogenesis of AK and SCC, including MAPK, PI3K–Akt, HIF-1α, Wnt, insulin, and ErbB signaling (Thomson et al., 2021). The MAPK pathway plays a crucial role in promoting the growth and survival of various malignancies (Fang and Richardson, 2005; Santarpia et al., 2012), and several studies suggest that the MAPK pathway may play a pivotal role in the transition from AK to SCC (Lambert et al., 2014; Zhang et al., 2018). These findings corroborate those of previous studies showing that curcumin downregulates p44/42 MAPK signaling and increases p53/p21 levels through the activation of p38 MAPK in UVB-exposed KCs (Ayli et al., 2010). Similarly, both PI3K–Akt and insulin signaling pathways are frequently altered in human cancers and serve to promote cell growth, survival, and metabolic processes by disconnecting the cell from control by exogenous growth signals (Hoxhaj and Manning, 2020; Malaguarnera and Belfiore, 2011). Aberrant insulin signaling may also promote a stem cell–like phenotype in malignant cells allowing

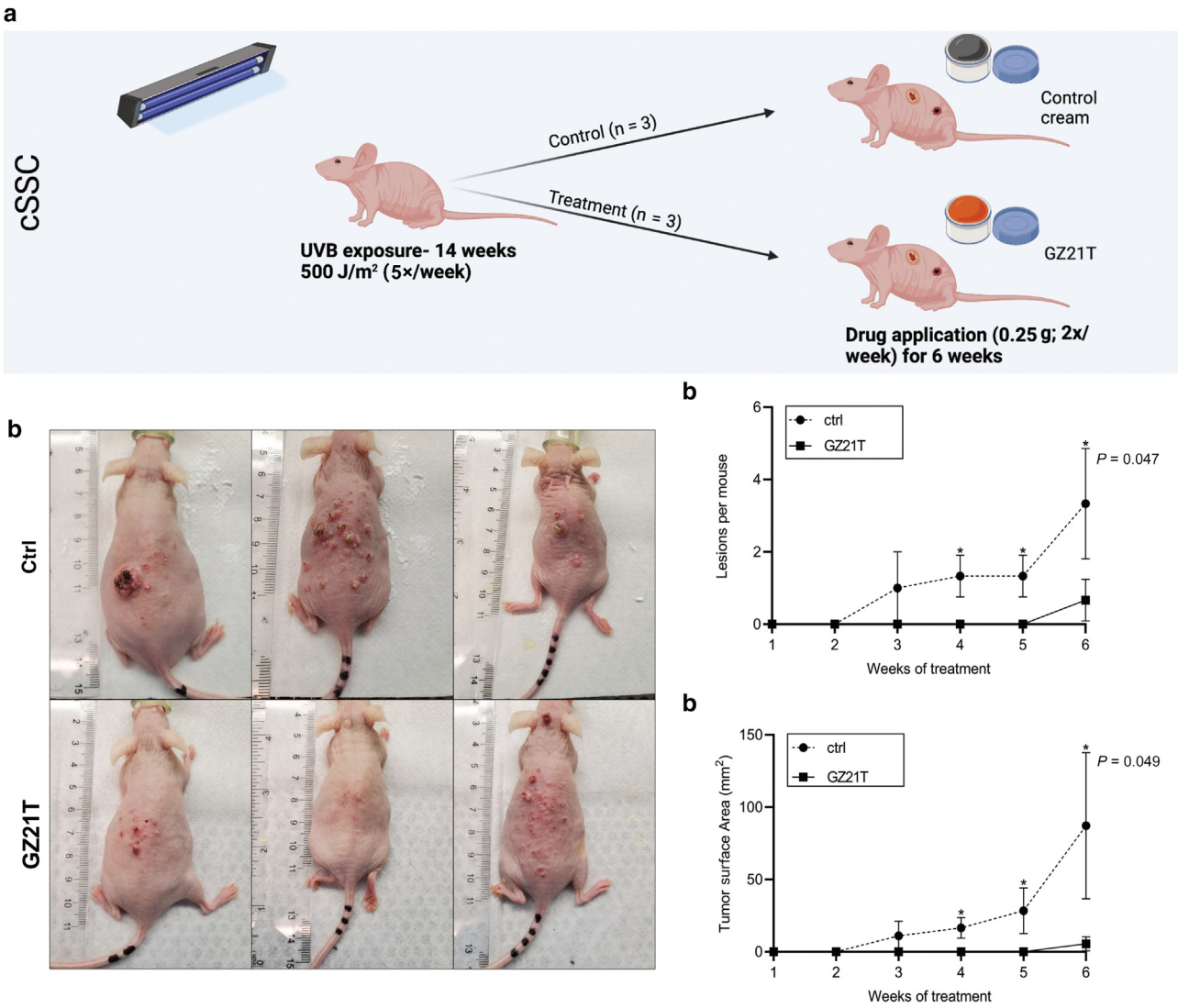

Figure 6. GZ21T inhibits the progression of actinic keratoses to cSCC. (**a**) To induce cSCC lesions, mice were irradiated with 500 J/m^2 5 days per week. Lesions developed after 14 weeks of irradiation, and mice were then treated with 0.25 g GZ21T (n = 3) or control cream (n = 3) two times per week for 6 weeks. This figure was created with biorender.com. (**b**) Representative images of control and GZ21T-treated mice after 6 weeks of treatment. (**c**) Count and (**d**) surface area of lesions >3 mm in diameter. Data points represent the mean, whereas error bars represent the SD. *$P < 0.05$. cSCC, cutaneous squamous cell carcinoma; ctrl, control.

for self-renewal and propagation of these tissues (Hoxhaj and Manning, 2020; Malaguarnera and Belfiore, 2011). Studies have shown that several key PI3K—Akt and insulin-like GF receptor proteins are overactivated in AK and become progressively more dysregulated with progression to cSCC, highlighting the role of these pathways in UV-induced skin carcinogenesis (Einspahr et al., 2012; Thomson et al., 2021). HIF-1α is a transcription factor that is activated by intratumoral hypoxia to promote angiogenesis, glucose metabolism, migration, and invasion (Balamurugan, 2016). In addition, overexpression of this protein has been associated with increased metastasis and higher mortality rates in several human cancers (Zhong et al., 1999; Zhou et al., 2006). The role of HIF-1α in AK specifically has been exemplified by murine-knockout models for the protein. Loss of HIF-1α results in decreased tumorigenesis as knockout mice exhibit an increased rate of DNA repair processes, slowing the accumulation of carcinogenic alterations (Mahfouf et al., 2019). Aberrant Wnt signaling has also been shown to be a major factor in cSCC development and progression as it allows the transcription factor β-catenin to escape proteasomal degradation to promote a stem-like phenotype and hyperproliferation of KCs (Lang et al., 2019). Finally, *ERBB* (*EGFR*) alterations are common in epithelial cancers because they provide a growth stimulus to promote self-renewal and propagation of malignant tissues (Ciardiello and Tortora, 2008). Previous studies have shown that numeric aberrations in EGFR expression may be present in up to 52% of AKs and 77% of cSCC (Toll et al., 2010). Interestingly, these pathways were not altered in NL skin, suggesting that GZ21T may preferentially suppress their signaling in AK lesions while sparing healthy tissue.

At the protein level, NL tissue was characterized by upregulation of the T-cell inhibitory protein PD-L1 (Ghosh et al.,

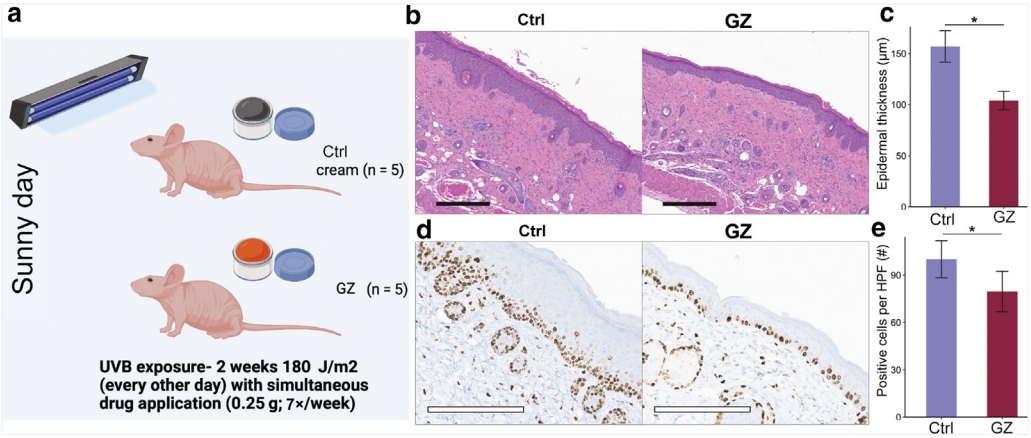

Figure 7. GZ exerts cytoprotective effects with short-term UV exposure. (**a**) To assess the histologic effects of GZ with short-term UV exposure, mice were irradiated with 180 J/m^2 each day for 2 weeks with simultaneous application of 0.25 g GZ (n = 5) or control cream (n = 5). This figure was created with biorender.com. (**b**) Representative H&E images of control and GZ-treated mice after 2 weeks of UV exposure and treatment. Black bars represent 300 μm. (**c**) Average epidermal thickness in control and GZ-treated mice. Bars represent the mean, whereas error bars represent the SEM. (**d**) Representative images of Ki-67 staining in control and GZ-treated mice after 2 weeks of UV exposure and treatment. White bars represent 200 μm. (**e**) Quantification of Ki-67 staining in control and GZ-treated mice. Bars represent the mean, whereas error bars represent the SEM. *$P < 0.05$. ctrl, control; GZ, GZ21T; HPF, high-powered field.

2021) and glutaminase, a metabolic enzyme that promotes tumorigenesis (Wang et al., 2020). Progression from PL to AK resulted in increased expression of pAkt1 S473, eEF2K, and LCN2, with suppression of RPA32 and FANCD2. These changes were reversed with GZ21T treatment. The findings in this study are in line with those of previous studies showing that GZ17-6.02 treatment enhances the efficacy of anti−PD-1 checkpoint inhibitors (Booth et al., 2020). pAkt1 S473 is increased in several head and neck squamous cell carcinomas (Islam et al., 2014) and promotes aberrant proliferation and survival of AK through the PI3K−Akt pathway. Both eEF2K and LCN2 have been found to promote migration and invasion of cancer cells in esophageal squamous cell carcinomas (Du et al., 2015; Islam et al., 2014; Zhu et al., 2015) and may support the survival of neoplastic tissue under conditions of nutrient deprivation (Temme and Asquith, 2021). Meanwhile, RPA32 and FANCD2 play a key role in DNA repair and DNA damage checkpoint responses (Alcón et al., 2020; Zou et al., 2006). Their upregulation suggests that GZ21T suppresses AK development by reducing the accumulation of carcinogenic alterations after UVB exposure. Finally, we found that GZ21T upregulates AMPK, a protein that promotes autophagy by phosphorylating proteins within the ULK1 and mTORC1 complexes (Li and Chen, 2019). This finding corroborates those of previous studies showing that GZ17-6.02 promotes the death of AK cells by upregulating the autophagic flux (West et al., 2022). Taken together, the findings from transcriptomic and proteomic analyses indicate that GZ21T affects a wide range of cellular targets, and its ability to inhibit AK growth is likely multifactorial.

Finally, our in vivo data also show a robust inhibition in the progression of lesions >3 mm in diameter and a reduction in epidermal thickness and the number of Ki-67−positive cells with short-term UV exposure. Increased KC proliferation is an adaptive response to UV damage that may eventually aid in the accumulation of allelic variation and progression to AK (Marionnet et al., 2014). As such, the findings in this study suggest that GZ21T exerts a cytoprotective effect in response to short-term UV exposure leading to a decrease in KC proliferation in response to UV damage.

Limitations of this study include its small sample size and testing only in mice. Furthermore, the hairless mice used in this study lack the hairless transcription factor, which may increase their propensity to develop cutaneous neoplasms in response to UV exposure as hairlessness promotes differentiation and inhibits proliferation of KCs (Kim et al., 2012; Panteleyev et al., 2000; Thompson et al., 2006). Hairlessness has not been shown to be altered in human AKs/cSCC. The model utilized in this study may thus not perfectly represent the biology of human AKs. The UV lamps used in this study also produce small amounts of UVA and UVC radiation. These wavelengths were not filtered, and GZ21T's effect on their contribution to carcinogenesis was not evaluated. Finally, mice in the short-term UV experiment were not followed longitudinally to quantify AK development, nor were experiments performed to evaluate allelic variation burden. The decreased epidermal thickness observed in these experiments may be partially due to the antiproliferative effects of GZ21T and may not directly indicate a protective effect with respect to transformation. Future studies should be conducted to test GZ21T's efficacy in other models and humans. In conclusion, GZ21T inhibits the growth of AKs by modulating the key drivers of multiple pathways such as MAPK, PI3K−Akt, Wnt, and ERBB signaling and represents a promising therapeutic option for the treatment of AKs.

MATERIALS AND METHODS

Ethical statement

All animal protocols used in this study were approved and performed in accordance with guidelines set forth by the Duke University Institutional Animal Care and Use Committee under protocol number A155-20-07.

Chemicals and reagents

GZ21T and control cream were provided by Genzada Pharmaceuticals (Hutchinson, KS). GZ21T was developed commercially

utilizing excipients well-characterized and approved by the Food and Drug Administration and European Medicines Agency. Unpublished data show the penetration of active pharmaceutical ingredients into the epidermis and, to a lesser degree, the dermis. The formulation has also been optimized for long-term stability.

Animal experiments

For induction of AK lesions, female SKH1 mice (Charles River Laboratories, Wilmington, MA) aged between 6 and 8 weeks were irradiated with 500 J/m^2 (the minimum erythemal dose [Pillon et al., 2017]) UVB 5 days per week for 10 weeks, using a Phillips TL 40W12 RS SLV/25 fluorescent tube (number 928011301230, Phillips, Eindhoven, The Netherlands) mounted 25 cm above the floor of a dedicated enclosure (Choi et al., 2022b). Power output was measured using a PM100D power meter and S120VC power sensor (number S120VC, Thorlabs, Newton, NJ) and was used to calculate the exposure time. Exposure times were internally recalibrated every week to account for temporal power degradation. Mice were monitored daily for signs of cutaneous injury. After the 10-week irradiation period, mice were randomized into control and treatment groups. Mice in the control group were treated with 0.25 g topical placebo cream 5 days per week, whereas mice in the treatment group received 0.25 g topical GZ21T 5 days per week. For all animal experiments, both placebo cream and GZ21T were applied to the irradiated backs. Mice were treated for 8 weeks. Lesions were measured using digital calipers, and tumor burden was quantified as total lesion count and the surface area occupied by the tumor.

To evaluate the ability of GZ21T to prevent the progression of AK to cSCC, female SKH1 mice aged between 6 and 8 weeks were irradiated with 500 J/m^2 UVB 5 days per week. After 14 weeks, mice began to develop lesions and were randomized into control and treatment groups. Mice then received 0.25 g topical control cream (control) or GZ21T (treatment) twice weekly for 6 weeks. The dosing frequency was reduced compared with that in the AK experiment to determine whether GZ21T could exert antitumor activity with less frequent application. Tumor burden of lesions likely to be cSCC was assessed using the total count and surface area occupied by lesions >3 mm in diameter because lesions of this size are more likely to represent cSCC than AK (de Gruijl and van der Leun, 1991).

To assess the short-term histopathologic effects of GZ21T on UVB-induced epidermal proliferation, female SKH1 mice aged between 6 and 8 weeks were exposed to UVB (180 mJ/cm^2) every other day for 2 weeks, which mimics sun exposure during a sunny vacation (Mintie et al., 2020). Mice in the control group were treated with 0.25 g topical placebo cream daily, whereas mice in the treatment group were treated with 0.25 g topical GZ21T.

mRNA sequencing

Lesional samples were collected from AK lesions, PL samples were taken from skin immediately adjacent to a lesional area, NL samples were collected from normal-appearing skin at least 5 cm away from a lesional area, and non-UV–exposed samples were collected from the skin on the ventral surface. All skin samples were flash frozen in liquid nitrogen and stored at −80 °C. Total RNA was isolated using an RNAeasy plus kit (number 74034, Qiagen, Hilden, Germany) according to the manufacturer's instructions. RNA-sequencing data were processed using the TrimGalore toolkit (https://www.bioinformatics.babraham.ac.uk/projects/trim_galore). Rsem-1.3.0 was used for alignments and generating gene and isoform expression levels. Reads were mapped to the GRCm38 version of the mouse genome and transcriptome. Reads were kept for subsequent analysis if they mapped to a single genomic location. Normalization and differential expression were carried out using the DESeq2 (Love et al., 2014) Bioconductor (Huber et al., 2015) package with the R statistical programming environment (www.r-project.org). The false discovery rate was calculated to control for multiple hypothesis testing. GSEA was performed using the GSEA software (Mootha et al., 2003; Subramanian et al., 2005), with the Kyoto Encyclopedia of Genes and Genomes database as a reference. Gene set variation analysis was conducted with the GSVA R Bioconductor package using the R statistical programming environment (Hänzelmann et al., 2013). DEGs were defined as coding genes with a log fold change > 1 or ≤ 1 and a false discovery rate–adjusted $P < 0.05$.

RPPA

Lesional, PL, NL, and non-UV–exposed skin were collected from mice, flash frozen in liquid nitrogen, and stored at −80 °C before being sent to MD Anderson's RPPA core facility for processing. Kyoto Encyclopedia of Genes and Genomes functional enrichment analyses were performed on gene lists of proteins whose expression decreased with GZ21T treatment using enrichR (Chen et al., 2013; Kuleshov et al., 2016; Xie et al., 2021). The full output of RPPA used in these experiments is provided in the Supplementary Files.

Histologic assessment

At the end of the in vivo experiments, mice were killed, and dorsal skin samples were fixed in 10% neutral-buffered formalin. Formalin-fixed tissues were paraffin embedded, sectioned, and mounted on serial slides at the Research Immunohistochemistry Laboratory at Duke University School of Medicine (Durham, SC). Slides were stained with H&E for histologic determination.

Immunohistochemistry

Ki-67 staining was performed using a rabbit Ki-67 antibody (number ab16667, Abcam, Cambridge, United Kingdom) at a 1:200 dilution with Discovery Antibody Diluent (number 760-108, Roche, Basel, Switzerland). Immunohistochemistry tests were performed using the Ultra Discovery automated staining platform (number 05987750001, Roche). Tissue sections were pretreated with Roche cell conditioning solution CC1 (number 950-124, Roche) for 56 minutes and were subsequently incubated with rabbit monoclonal Ki-67 for 60 minutes at 36 °C. Rabbit IgG, substituted for the primary antibody, was used as a negative control. After binding of the primary antibody, Roche anti-rabbit HQ (number 760-4815, Roche) was applied and incubated for 12 minutes, followed by a 12-minute incubation with anti-HQ horseradish peroxidase (number 760-4820, Roche) for antigen detection. The immunohistochemistry reaction was visualized with 3,3′-diaminobenzidine chromogen and counterstained hematoxylin.

Statistical analysis

Statistical analyses were conducted using GraphPad Prism 9.0 (GraphPad Software, San Diego, CA). Gene set variation analysis scores were compared using the limma package for R, version 4.1.2. *P*-values for GSEA and gene set variation analysis were adjusted using the Benjamini–Hochberg method. Comparisons between all other groups were made using the Student's *t*-test or the Mann–Whitney *U* test for normally and non-normally distributed data, respectively. Normality was assessed using the Shapiro–Wilk test. Differences with a *P*-value or adjusted $P < 0.05$ were considered statistically significant.

Data availability statement

The data that support the findings of this study are available from the Gene Expression Omnibus under GSE223986 or the Supplementary Files.

ORCIDs

Zachary A. Bordeaux: http://orcid.org/0000-0002-8833-6080
Justin Choi: http://orcid.org/0000-0002-8388-6876
Gabrielle Braun: http://orcid.org/0000-0003-4496-3696
Cole Davis: http://orcid.org/0000-0003-0253-8720
Melika Marani: http://orcid.org/0000-0002-6584-9457
Kevin Lee: http://orcid.org/0000-0001-7559-5529
Christeen Samuel: http://orcid.org/000-001-9798-1463
Jackson Adams: http://orcid.org/0000-0002-4555-2488
Reed Windom: http://orcid.org/0000-0003-2024-6799
Anthony Pollizzi: http://orcid.org/0000-0002-2780-2746
Anusha Kambala: http://orcid.org/0000-0002-0350-8622
Hannah Cornman: http://orcid.org/0000-0003-1462-2479
Sriya V. Reddy: http://orcid.org/0000-0002-7584-7594
Weiying Lu: http://orcid.org/0000-0003-1539-2708
Martin P. Alphonse: http://orcid.org/0000-0003-3447-1284
Cameron E. West: http://orcid.org/0000-0001-9673-9165
Shawn G. Kwatra: http://orcid.org/0000-0003-3736-1515
Madan M. Kwatra: http://orcid.org/0000-0002-6547-8852

CONFLICT OF INTEREST

SGK is an advisory board member/consultant for AbbVie, Aslan Pharmaceuticals, Arcutis Biotherapeutics, Celldex Therapeutics, Galderma, Genzada Pharmaceuticals, Incyte, Johnson & Johnson, Novartis Pharmaceuticals, Pfizer, Regeneron Pharmaceuticals, and Sanofi and has served as an investigator for Galderma, Incyte, Pfizer, and Sanofi. CEW is an officer of and member of the Board of Directors at Genzada Pharmaceuticals. The remaining authors state no conflict of interest.

ACKNOWLEDGMENTS

Funding for this study was provided by Genzada Pharmaceuticals.

AUTHOR CONTRIBUTIONS

Conceptualization: ZAB, JC, CEW, SGK, MMK; Data Curation: ZAB, JC, GB, CD; Formal Analysis: ZAB, JC; Funding Acquisition: MMK; Investigation: ZAB, JC, GB, CD, CEW, SGK, MMK; Methodology: ZAB, JC, CEW, SGK, MMK; Project Administration: CEW, SGK, MMK; Resources: CEW, SGK, MMK; Software: ZAB, JC; Supervision: CEW, SGK, MMK; Validation: CEW, SGK, MMK; Visualization: ZAB, JC; Writing — Original Draft Preparation: ZAB, JC, MM, KL, CS, CEW, SGK, MMK; Writing — Review and Editing: ZAB, JC, GB, CD, MM, KL, CS, JA, RW, AP, AK, HC, SVR, WL, OOO, MPA, CEW, SGK, MMK

Disclaimer

The funding organization took no part in data acquisition for this study.

SUPPLEMENTARY MATERIAL

Supplementary material is linked to the online version of the paper at www.jidonline.org, and at https://doi.org/10.1016/j.jid.2023.100206.

REFERENCES

Alcón P, Shakeel S, Chen ZA, Rappsilber J, Patel KJ, Passmore LA. FANCD2-FANCI is a clamp stabilized on DNA by monoubiquitination of FANCD2 during DNA repair. Nat Struct Mol Biol 2020;27:240–8.

Arenberger P, Arenbergerova M. New and current preventive treatment options in actinic keratosis. J Eur Acad Dermatol Venereol 2017;31(Suppl 5):13–7.

Ayli EE, Dugas-Breit S, Li W, Marshall C, Zhao L, Meulener M, et al. Curcuminoids activate p38 MAP kinases and promote UVB-dependent signalling in keratinocytes. Exp Dermatol 2010;19:493–500.

Balamurugan K. HIF-1 at the crossroads of hypoxia, inflammation, and cancer. Int J Cancer 2016;138:1058–66.

Berman B, Cockerell CJ. Pathobiology of actinic keratosis: ultraviolet-dependent keratinocyte proliferation. J Am Acad Dermatol 2013;68:S10–9.

Boone MA, Suppa M, Marneffe A, Miyamoto M, Jemec GB, Del Marmol V. A new algorithm for the discrimination of actinic keratosis from normal skin and squamous cell carcinoma based on in vivo analysis of optical properties by high-definition optical coherence tomography. J Eur Acad Dermatol Venereol 2016;30:1714–25.

Booth L, Roberts JL, West C, Dent P. GZ17-6.02 kills prostate cancer cells in vitro and in vivo. Front Oncol 2022b;12:1045459.

Booth L, Roberts JL, West C, Von Hoff D, Dent P. GZ17-6.02 initiates DNA damage causing autophagosome-dependent HDAC degradation resulting in enhanced anti-PD1 checkpoint inhibitory antibody efficacy. J Cell Physiol 2020;235:8098–113.

Booth L, West C, Moore RP, Von Hoff D, Dent P. GZ17-6.02 and palbociclib interact to kill ER+ breast cancer cells. Oncotarget 2022a;13:92–104.

Booth L, West C, Von Hoff D, Kirkwood JM, Dent P. GZ17-6.02 interacts with [MEK1/2 and B-RAF inhibitors] to kill melanoma cells. Front Oncol 2021;11:656453.

Bordeaux ZA, Kwatra SG, Booth L, Dent P. A novel combination of isovanillin, curcumin, and harmine (GZ17-6.02) enhances cell death and alters signaling in actinic keratoses cells when compared to individual components and two-component combinations. Anticancer Drugs 2023;34:544–50.

Brennan CW, Verhaak RG, McKenna A, Campos B, Noushmehr H, Salama SR, et al. The somatic genomic landscape of glioblastoma [published correction appears in Cell 2014;157:753] Cell 2013;155:462–77.

Chamcheu JC, Roy T, Uddin MB, Banang-Mbeumi S, Chamcheu RN, Walker AL, et al. Role and therapeutic targeting of the PI3K/Akt/mTOR signaling pathway in skin cancer: a review of current status and future trends on natural and synthetic agents therapy. Cells 2019;8:803.

Chen A, Xu J, Johnson AC. Curcumin inhibits human colon cancer cell growth by suppressing gene expression of epidermal growth factor receptor through reducing the activity of the transcription factor Egr-1. Oncogene 2006;25:278–87.

Chen EY, Tan CM, Kou Y, Duan Q, Wang Z, Meirelles GV, et al. Enrichr: interactive and collaborative HTML5 gene list enrichment analysis tool. BMC Bioinformatics 2013;14:128.

Choi J, Bordeaux ZA, Braun G, Davis C, Parthasarathy V, Deng J, et al. Construction of a secondary enclosure for UVB irradiation of mice. JID Innov 2022b;3:100107.

Choi J, Bordeaux ZA, McKeel J, Nanni C, Sutaria N, Braun G, et al. GZ17-6.02 inhibits the growth of EGFRvIII+ glioblastoma. Int J Mol Sci 2022a;23:4174.

Ciardiello F, Tortora G. EGFR antagonists in cancer treatment [published correction appears in N Eng J Med 2009;360:1579] N Engl J Med 2008;358:1160–74.

Costa C, Scalvenzi M, Ayala F, Fabbrocini G, Monfrecola G. How to treat actinic keratosis? An update. J Dermatol Case Rep 2015;9:29–35.

de Gruijl FR, van der Leun JC. Development of skin tumors in hairless mice after discontinuation of ultraviolet irradiation. Cancer Res 1991;51:979–84.

Dirschka T, Gupta G, Micali G, Stockfleth E, Basset-Séguin N, Del Marmol V, et al. Real-world approach to actinic keratosis management: practical treatment algorithm for office-based dermatology. J Dermatolog Treat 2017;28:431–42.

Du ZP, Wu BL, Xie YM, Zhang YL, Liao LD, Zhou F, et al. Lipocalin 2 promotes the migration and invasion of esophageal squamous cell carcinoma cells through a novel positive feedback loop. Biochim Biophys Acta 2015;1853:2240–50.

Einspahr JG, Calvert V, Alberts DS, Curiel-Lewandrowski C, Warneke J, Krouse R, et al. Functional protein pathway activation mapping of the progression of normal skin to squamous cell carcinoma [published correction appears in Cancer Prev Res (Phila) 2012;5:1072] Cancer Prev Res (Phila) 2012;5:403–13.

Fang JY, Richardson BC. The MAPK signalling pathways and colorectal cancer. Lancet Oncol 2005;6:322–7.

Fernandez Figueras MT. From actinic keratosis to squamous cell carcinoma: pathophysiology revisited. J Eur Acad Dermatol Venereol 2017;31(Suppl 2):5–7.

Flohil SC, van der Leest RJT, Dowlatshahi EA, Hofman A, de Vries E, Nijsten T. Prevalence of actinic keratosis and its risk factors in the general population: the Rotterdam Study. J Invest Dermatol 2013;133:1971–8.

Ghosh C, Luong G, Sun Y. A snapshot of the PD-1/PD-L1 pathway. J Cancer 2021;12:2735–46.

Ghosh C, Paul S, Dandawate P, Gunewardena SS, Subramaniam D, West C, et al. Super-enhancers: novel target for pancreatic ductal adenocarcinoma. Oncotarget 2019;10:1554–71.

Hänzelmann S, Castelo R, Guinney J. GSVA: gene set variation analysis for microarray and RNA-Seq data. BMC Bioinformatics 2013;14:7.

Helson L. Curcumin (diferuloylmethane) delivery methods: a review. BioFactors 2013;39:21–6.

Hoxhaj G, Manning BD. The PI3K-AKT network at the interface of oncogenic signalling and cancer metabolism. Nat Rev Cancer 2020;20:74–88.

Huber W, Carey VJ, Gentleman R, Anders S, Carlson M, Carvalho BS, et al. Orchestrating high-throughput genomic analysis with Bioconductor. Nat Methods 2015;12:115–21.

Islam MR, Ellis IR, Macluskey M, Cochrane L, Jones SJ. Activation of Akt at T308 and S473 in alcohol, tobacco and HPV-induced HNSCC: is there evidence to support a prognostic or diagnostic role? Exp Hematol Oncol 2014;3:25.

Kim H, Casta A, Tang X, Luke CT, Kim AL, Bickers DR, et al. Loss of hairless confers susceptibility to UVB-induced tumorigenesis via disruption of NF-kappaB signaling. PLoS One 2012;7:e39691.

Kuleshov MV, Jones MR, Rouillard AD, Fernandez NF, Duan Q, Wang Z, et al. Enrichr: a comprehensive gene set enrichment analysis web server 2016 update. Nucleic Acids Res 2016;44:W90–7.

Lambert SR, Mladkova N, Gulati A, Hamoudi R, Purdie K, Cerio R, et al. Key differences identified between actinic keratosis and cutaneous squamous cell carcinoma by transcriptome profiling. Br J Cancer 2014;110:520–9.

Lang CMR, Chan CK, Veltri A, Lien WH. Wnt signaling pathways in keratinocyte carcinomas. Cancers (Basel) 2019;11:1216.

Li Y, Chen Y. AMPK and autophagy. Adv Exp Med Biol 2019;1206:85–108.

Love MI, Huber W, Anders S. Moderated estimation of fold change and dispersion for RNA-seq data with DESeq2. Genome Biol 2014;15:550.

Mahfouf W, Hosseini M, Muzotte E, Serrano-Sanchez M, Dousset L, Moisan F, et al. Loss of epidermal HIF-1α blocks UVB-induced tumorigenesis by affecting DNA repair capacity and oxidative stress [published correction appears in J Invest Dermatol 2022;142:1506–7] J Invest Dermatol 2019;139:2016–28.e7.

Maiti P, Scott J, Sengupta D, Al-Gharaibeh A, Dunbar GL. Curcumin and solid lipid curcumin particles induce autophagy, but inhibit mitophagy and the PI3K-Akt/mTOR pathway in cultured glioblastoma cells. Int J Mol Sci 2019;20:399.

Malaguarnera R, Belfiore A. The insulin receptor: a new target for cancer therapy. Front Endocrinol (Lausanne) 2011;2:93.

Marionnet C, Tricaud C, Bernerd F. Exposure to non-extreme solar UV daylight: spectral characterization, effects on skin and photoprotection. Int J Mol Sci 2014;16:68–90.

Mintie CA, Musarra AK, Singh CK, Ndiaye MA, Sullivan R, Eickhoff JC, et al. Protective effects of dietary grape on UVB-mediated cutaneous damages and skin tumorigenesis in SKH-1 mice. Cancers (Basel) 2020;12:1751.

Mootha VK, Lindgren CM, Eriksson KF, Subramanian A, Sihag S, Lehar J, et al. PGC-1α-responsive genes involved in oxidative phosphorylation are coordinately downregulated in human diabetes. Nat Genet 2003;34:267–73.

Panteleyev AA, Paus R, Christiano AM. Patterns of hairless (hr) gene expression in mouse hair follicle morphogenesis and cycling. Am J Pathol 2000;157:1071–9.

Pillon A, Gomes B, Vandenberghe I, Cartron V, Cèbe P, Blanchet JC, et al. Actinic keratosis modelling in mice: a translational study. PLoS One 2017;12:e0179991.

Pozo N, Zahonero C, Fernández P, Liñares JM, Ayuso A, Hagiwara M, et al. Inhibition of DYRK1A destabilizes EGFR and reduces EGFR-dependent glioblastoma growth. J Clin Invest 2013;123:2475–87.

Ratushny V, Gober MD, Hick R, Ridky TW, Seykora JT. From keratinocyte to cancer: the pathogenesis and modeling of cutaneous squamous cell carcinoma. J Clin Invest 2012;122:464–72.

Salmon N, Tidman MJ. Managing actinic keratosis in primary care. Practitioner 2016;260:25–9.

Santarpia L, Lippman SM, El-Naggar AK. Targeting the MAPK-RAS-RAF signaling pathway in cancer therapy. Expert Opin Ther Targets 2012;16:103–19.

Subramanian A, Tamayo P, Mootha VK, Mukherjee S, Ebert BL, Gillette MA, et al. Gene set enrichment analysis: a knowledge-based approach for interpreting genome-wide expression profiles. Proc Natl Acad Sci USA 2005;102:15545–50.

Sun XD, Liu XE, Huang DS. Curcumin induces apoptosis of triple-negative breast cancer cells by inhibition of EGFR expression. Mol Med Rep 2012;6:1267–70.

Taute S, Pfister HJ, Steger G. Induction of tyrosine phosphorylation of UV-activated EGFR by the beta-human papillomavirus Type 8 E6 leads to papillomatosis. Front Microbiol 2017;8:2197.

Temme L, Asquith CRM. eEF2K: an atypical kinase target for cancer. Nat Rev Drug Discov 2021;20:577.

Thompson CC, Sisk JM, Beaudoin GM 3rd. Hairless and Wnt signaling: allies in epithelial stem cell differentiation. Cell Cycle 2006;5:1913–7.

Thomson J, Bewicke-Copley F, Anene CA, Gulati A, Nagano A, Purdie K, et al. The genomic landscape of actinic keratosis. J Invest Dermatol 2021;141:1664–74.e7.

Toll A, Salgado R, Yébenes M, Martín-Ezquerra G, Gilaberte M, Baró T, et al. Epidermal growth factor receptor gene numerical aberrations are frequent events in actinic keratoses and invasive cutaneous squamous cell carcinomas. Exp Dermatol 2010;19:151–3.

Vallianou NG, Evangelopoulos A, Schizas N, Kazazis C. Potential anticancer properties and mechanisms of action of curcumin. Anticancer Res 2015;35:645–51.

Vishwakarma V, New J, Kumar D, Snyder V, Arnold L, Nissen E, et al. Potent antitumor effects of a combination of three nutraceutical compounds. Sci Rep 2018;8:12163.

Vollono L, Falconi M, Gaziano R, Iacovelli F, Dika E, Terracciano C, et al. Potential of curcumin in skin disorders. Nutrients 2019;11:2169.

Wang Z, Liu F, Fan N, Zhou C, Li D, Macvicar T, et al. Targeting glutaminolysis: new perspectives to understand cancer development and novel strategies for potential target therapies. Front Oncol 2020;10:589508.

West CE, Kwatra SG, Choi J, Von Hoff D, Booth L, Dent P. A novel plant-derived compound is synergistic with 5-fluorouracil and has increased apoptotic activity through autophagy in the treatment of actinic keratoses. J Dermatolog Treat 2022;33:590–1.

Xie Z, Bailey A, Kuleshov MV, Clarke DJB, Evangelista JE, Jenkins SL, et al. Gene set knowledge discovery with Enrichr. Curr Protoc 2021;1:e90.

Zhang L, Li D, Yu S. Pharmacological effects of harmine and its derivatives: a review. Arch Pharm Res 2020;43:1259–75.

Zhang L, Qin H, Wu Z, Chen W, Zhang G. Pathogenic genes related to the progression of actinic keratoses to cutaneous squamous cell carcinoma. Int J Dermatol 2018;57:1208–17.

Zhen L, Fan D, Yi X, Cao X, Chen D, Wang L. Curcumin inhibits oral squamous cell carcinoma proliferation and invasion via EGFR signaling pathways. Int J Clin Exp Pathol 2014;7:6438–46.

Zhong H, De Marzo AM, Laughner E, Lim M, Hilton DA, Zagzag D, et al. Overexpression of hypoxia-inducible factor 1alpha in common human cancers and their metastases. Cancer Res 1999;59:5830–5.

Zhou J, Schmid T, Schnitzer S, Brüne B. Tumor hypoxia and cancer progression. Cancer Lett 2006;237:10–21.

Zhu H, Yang X, Liu J, Zhou L, Zhang C, Xu L, et al. Eukaryotic elongation factor 2 kinase confers tolerance to stress conditions in cancer cells. Cell Stress Chaperones 2015;20:217–20.

Zou Y, Liu Y, Wu X, Shell SM. Functions of human replication protein A (RPA): from DNA replication to DNA damage and stress responses. J Cell Physiol 2006;208:267–73.